JOURNAL OF BACTERIOLOGY, Oct. 1988, p. 4681–4692
0021-9193/88/104681-12$02.00/0

Vol. 170, No. 10

In Vivo Analysis of *puf* Operon Expression in *Rhodobacter sphaeroides* after Deletion of a Putative Intercistronic Transcription Terminator

BRADLEY S. DEHOFF,[1]† JEONG K. LEE,[1] TIMOTHY J. DONOHUE,[2] RICHARD I. GUMPORT,[3] AND SAMUEL KAPLAN[1]*

Departments of Microbiology[1] and Biochemistry,[3] University of Illinois at Urbana-Champaign, Urbana, Illinois 61801, and Bacteriology Department, University of Wisconsin, Madison, Wisconsin 53706[2]

Received 31 May 1988/Accepted 7 July 1988

The intercistronic region of the mRNA derived from the *puf* operon of *Rhodobacter sphaeroides* is capable of forming two stable stem-loop structures, the first of which resembles a factor-independent transcription terminator. A *puf* operon construction lacking the putative transcription terminator was made in vitro and crossed into the chromosome of *R. sphaeroides* PUFB1 to yield a single chromosomal copy in the terminator-deleted strain. The mutant strain, designated PUFΔ348-420 which was otherwise isogenic with the wild-type strain 2.4.1, showed a normal growth rate at high light intensity compared with the wild type, with the levels of the B875 and reaction center spectral complexes being approximately 7% and 25%, respectively, of those found in the wild type. The deletion mutation correlated with a reduction in the size of the fixed photosynthetic unit from 15:1 in the wild type to 4:1 in the mutant. The level of the B800-850 complex was increased approximately twofold in the mutant strain. However, substantial amounts of the B875 and reaction center polypeptides were not incorporated into spectrally active complexes, suggesting the importance of other factors in the assembly of these complexes. Removal of the intercistronic stem-loops resulted in increased readthrough of the *puf* operon terminator to regions downstream, as well as altering the stability of the resulting *puf* operon-specific transcripts. A model is proposed which links ribosome stalling within the open reading frame *K* leader region of the *puf* operon transcript with chain termination.

Rhodobacter sphaeroides is a purple nonsulfur photosynthetic bacterium capable of growth under diverse physiological conditions, including both chemoheterotrophic and photoheterotrophic growth. When growing photosynthetically, *R. sphaeroides* synthesizes an intracytoplasmic membrane system that contains all the necessary components for primary photochemistry. These include the B800-850 and B875 light-harvesting complexes that function to absorb light energy and transfer it to the reaction center (RC) (31). The ratio of the B800-850 to RC complexes found in isolated intracytoplasmic membrane varies inversely with the incident light intensity used for growth, whereas the ratio of B875 to RC is fixed at approximately 15:1 and is independent of light intensity (1).

The genes encoding the B875 polypeptides, as well as the RC-L and RC-M polypeptides, have recently been identified and are clustered in a transcriptional unit, designated the *puf* operon (20, 47, 48). The genes encoding the B875 β and α polypeptides, *pufB* and *pufA*, respectively, are proximal to the genes encoding the RC-L and RC-M polypeptides, *pufL* and *pufM*, respectively.

Recently, an open reading frame (ORF) (designated *pufX*) located immediately downstream of *pufM* and capable of encoding an 82-amino-acid polypeptide has been sequenced (J. K. Lee, B. S. DeHoff, R. Gyure, T. J. Donohue, R. I. Gumport, and S. Kaplan, manuscript in preparation). One transcript of 0.5 kilobases (kb) derived from the *puf* operon encodes the structural genes for the B875 β and α polypeptides. A larger transcript of 2.6 kb, recently identified as being approximately 2.7 kb by sequence analysis and S1 nuclease mapping (Lee et al., in preparation), also encodes the B875 β and α polypeptides, as well as the distal RC-L and RC-M polypeptides (53), and it includes the *pufX* ORF. Additionally, a third minor transcript, of 0.7 kb, terminating within the proximal region of the *pufL* gene has been detected. The ratio of the 0.5-kb transcript to the 2.7-kb transcript is between 8:1 and 15:1 under photosynthetic conditions and has been attributed to transcriptional regulation (53). The ratio of B875 to RC complexes under photosynthetic growth conditions would thus be regulated at the transcriptional level.

In addition to transcriptional control, the steady-state levels of mRNA species depend on the stability of mRNAs in procaryotes, which may be enhanced by the presence of regions of dyad symmetry capable of forming strong RNA stem-loop structures at their 3′ ends (36). Such regions have also been proposed to stabilize upstream mRNA derived from the degradation of a larger transcript (40). Additionally, G+C-rich stem-loop structures followed by uracil residues may act as *rho*-independent transcription terminators (2). The intercistronic region between *pufBA* and *pufLMX* contains two potential stem-loop structures, one of which resembles a *rho*-independent transcription terminator with a G+C-rich hairpin followed by the sequence -ATTC- (Fig. 1) (53).

We have deleted the putative transcription terminator residing in the intercistronic region of the *puf* operon from the chromosome of *R. sphaeroides* and have shown that the stability and ratios of the resulting *puf*-specific transcripts have changed during steady-state photoheterotrophic growth. We have also examined the physiological effects of this deletion on the light-harvesting and RC spectral com-

* Corresponding author.
† Present address: Eli Lilly and Company, Lilly Corporate Center, Indianapolis, IN 46285.

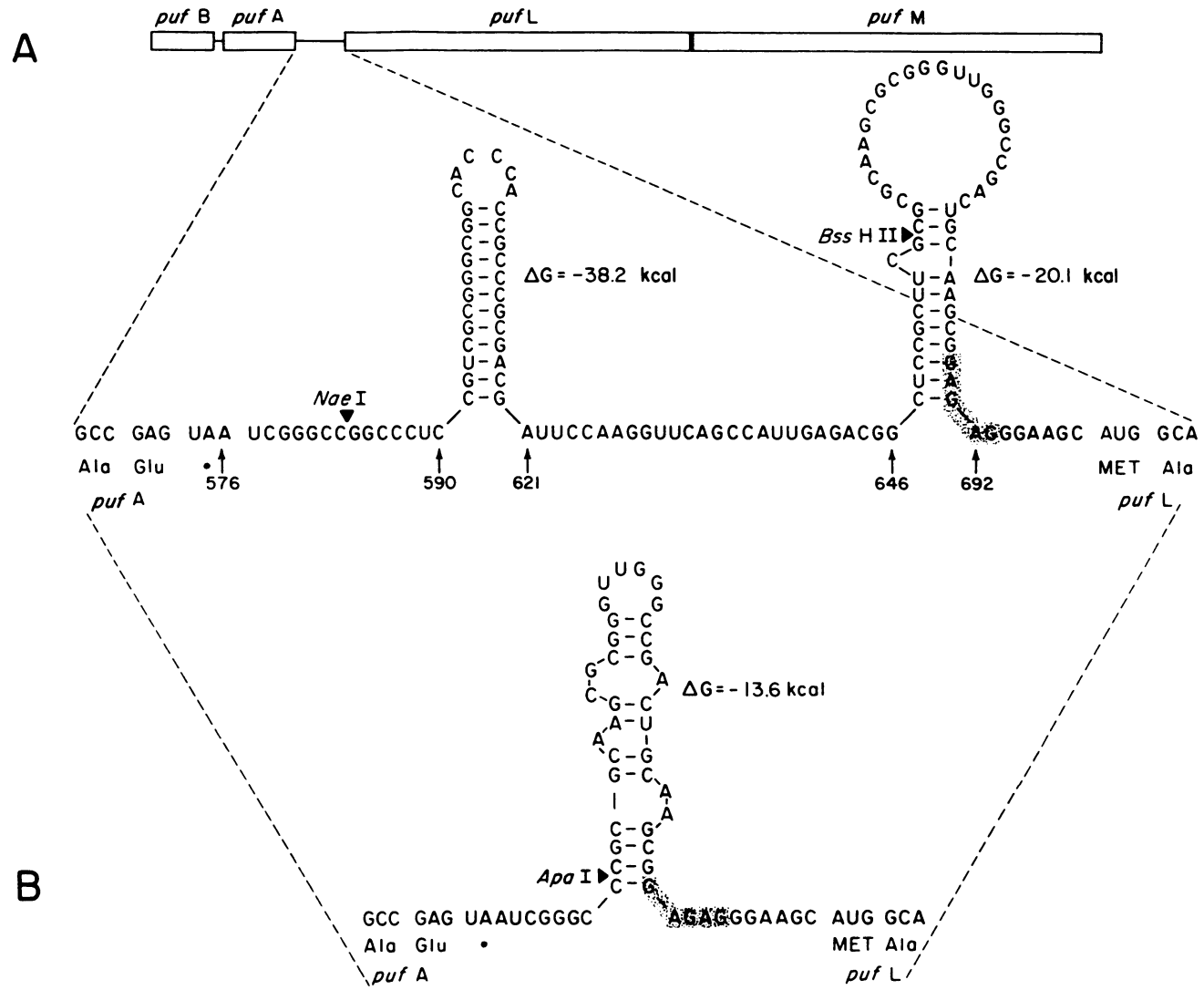

FIG. 1. Diagram of the proposed RNA secondary structures of the *puf* operon intercistronic region and a deleted derivative. (A) The upper portion shows the location of the relevant genes of the *puf* operon. The lower portion is the RNA sequence depicting the proposed intercistronic stem-loop structures. Restriction endonuclease recognition sites for the corresponding DNA sequence are also shown. (B) Proposed RNA secondary structure when the 73-bp *Nae*I-*Bss*HII fragment is deleted. An *Apa*I restriction endonuclease recognition site was created when the filled-in *Bss*HII site and the *Nae*I site were joined. The Gibb's free energy value for each proposed RNA stem-loop was calculated by the methods of Tinoco et al. (43). The proposed Shine-Dalgarno sequence for the *pufL* gene is shaded.

plexes and have quantified the amount of individual proteins present in the membrane by Western immunoblot analysis. Our results support the hypothesis that the proper stoichiometry of *puf* mRNAs provides the proper ratio of spectral complexes to functional RCs.

We also propose that the more 5′ proximal of the two stem-loop structures lying between *pufBA* and *pufLMX* acts as a transcription terminator when ribosome movement is uncoupled from RNA transcription. Readthrough of this terminator is proposed to occur when ribosome movement and RNA transcription proceed in tandem, but termination occurs when these processes are uncoupled due to ribosome stalling.

(A preliminary report of this work has been presented [B. S. DeHoff, J. K. Lee, T. J. Donohue, and R. I. Gumport, Abstr. Annu. Meet. Am. Soc. Microbiol. 1988, H-106, p. 162].)

MATERIALS AND METHODS

Bacterial strains, plasmids, and growth conditions. Bacterial strains and plasmid vectors are described in Table 1. *R. sphaeroides* strains were grown either chemoheterotrophically, photoheterotrophically, or under low oxygen conditions as previously described (10, 14, 27); special care was taken for RS103 growth (23). Cell growth was monitored by using a Klett-Summerson colorimeter (no. 66 filter) as described previously (41).

When necessary, kanamycin and tetracycline were added to Sistrom succinic acid minimal medium A (SSM) at final concentrations of 25 and 1 μg/ml, respectively, for selective conditions during growth of *R. sphaeroides* containing antibiotic resistance determinants. *E. coli* strains were grown at 37°C in Luria broth (28). Ampicillin and tetracyline (final concentrations, 25 and 15 μg/ml, respectively) were added to

TABLE 1. Bacterial strains and plasmids

Strain or plasmid	Relevant characteristic(s)	Source or reference
E. coli		
S17-1	Pro$^-$ Res$^-$ Mod$^+$ *recA*, integrated plasmid RP4-Tc::Mu-Km::Tn7	38
JM83	*ara* Δ(*lac-proAB*) *strA thi* φ80 *lacZ*ΔM15	33
R. sphaeroides		
2.4.1	Wild type	44
RS103	RS2 derivative (B875$^-$)	31
PUFB1	2.4.1 derivative (Puf$^-$ ORF Q^-) Km^r	10
PUFΔ348-420	2.4.1 derivative (deletion 348 to 420 bp from start of *pufB*)	This study
Plasmids		
pUC8	Ap^r	45
pUC19	Ap^r	50
pRK404	Tc^r	11
pBS	Ap^r, pUC19 with T3 and T7 promoters flanking polylinker	Stratagene
pUI710	Ap^r, pUC19/*Pst*I,*Kpn*I 1.30-kb *Pst*I-*Kpn*I (+)[a]	20
pUI580	Tc^r, pRK404/*Pst*I, 4.50-kb *Pst*I (−)	This study
pUI581	Tc^r, pRK404/*Pst*I, 4.50-kb *Pst*I (+)	This study
pUI900	Ap^r, pUC19/*Pst*I,*Kpn*I, 1.23-kb *Pst*I-*Kpn*I-(Δ)[b] (+)	This study
pUI902	Ap^r, pUC19/*Pst*I,[c] 4.43-kb *Pst*I-(Δ) (+)	This study
pUI904	Ap^r, pUC8/*Pst*I, 4.50-kb *Pst*I (−)	This study
pUI909	Tc^r, pRK404/*Pst*I, 4.43-kb *Pst*I-(Δ) (+)	This study
pUI910	Tc^r, pRK404/*Pst*I, 4.43-kb *Pst*I-(Δ) (−)	This study
pUI655	Ap^r, pBS/*Hin*cII, 0.48-kb *Sty*I[d] (−)[e]	This study
pUI662	Ap^r, pBS/*Hin*cII, 0.29-kb *Alu*I-*Pvu*II (−)[e]	This study
pUI658	Ap^r, pBS/*Sma*I,*Sal*I, 0.48-kb *Pvu*II-*Sal*I (−)[e]	This study
pUI663	Ap^r, pBS/*Sma*I, 0.49-kb *Nco*I-*Sma*I (+)[e]	This study

[a] (+), *puf* operon orientation is in the same direction as *lac* promoter; (−), opposite orientation.
[b] (Δ) denotes the 73-bp *Nae*I-*Bss*HII fragment deleted from *puf* intercistronic region.
[c] pUI902 does not contain the complete pUC19 polylinker (see Materials and Methods for the construction).
[d] 5′ overhangs were made blunt with DNA polymerase Klenow fragment.
[e] for pBS derivatives, (+) plasmid was linearized with *Hin*dIII and RNA probes were synthesized with T7 RNA polymerase; (−) plasmid was linearized with *Eco*RI and RNA probes were synthesized with T3 RNA polymerase.

E. coli cultures carrying plasmids encoding these drug resistance genes. When necessary, 5-bromo-4-chloro-3-indolyl-β-D-galactopyranoside (X-Gal) and isopropyl-β-D-thiogalactopyranoside (IPTG) were added at final concentrations of 40 μg/ml and 40 μM, respectively, when screening plasmid inserts for the absence of α-complementation.

Isolation of nucleic acids. Preparation of *R. sphaeroides* 2.4.1 genomic DNA has been described elsewhere (34). Highly purified plasmid DNA was isolated from *E. coli* JM83 (9) by the relaxation gradient method (17).

Triton X-100 lysates were prepared essentially as described by Maquat and Reznikoff (29). DNA was purified in a cesium chloride gradient formed by centrifugation in an 80 Ti rotor with Quick-Seal polyallomer centrifuge tubes (Beckman Instruments, Inc., Palo Alto, Calif.) at 20°C in a Sorvall RC80 ultracentrifuge (Du Pont Co. Biotechnology Systems, Wilmington, Del.) in step mode for 16 h at 57,000 rpm followed by a 1-h relaxation of the gradient at 40,000 rpm. Following centrifugation, fractions containing plasmid DNA were collected from the gradient and purified as described (28).

Small-scale plasmid preparations were obtained by the alkaline sodium dodecyl sulfate lysis method (4).

Genetic manipulations. *E. coli* strains were transformed with plasmid DNA by the method of Cohen et al. (8). The vector pRK404 (11) and its derivatives were introduced into *R. sphaeroides* by using the conjugation procedures previously described by Davis et al. (10).

Screening of exconjugants for sensitivity to RS1 bacteriophage. Exconjugants were screened for sensitivity to *R. sphaeroides*-specific RS1 bacteriophage by using the method of Donohue et al. (12) to confirm that all strains used in this study were *R. sphaeroides*.

Analysis of DNA samples and recombinant DNA techniques. Restriction fragments were separated by electrophoresis on 1.0% agarose or 5.0% polyacrylamide gels as described (9) and sized by using known standards (39). DNA fragments were purified from both agarose and acrylamide gels by electroelution followed by ethanol precipitation. Filling in of protruding 5′ ends to produce blunt ends and ligations of DNA fragments were performed as described (28).

The stem-loop structures within the intercistronic region of the *puf* operon were deleted by removing a 73-base-pair (bp) *Nae*I-*Bss*HII restriction fragment from pUI710, filling in the 5′ overhang of *Bss*HII, and ligating the blunt ends which formed an *Apa*I restriction site (Fig. 1). We confirmed the construction by restriction analysis; i.e., the joined ends were cleaved with *Apa*I (data not shown). A 4.5-kb *Pst*I fragment containing the *puf* operon was cloned into the *Pst*I site of pUC8, with the direction of the *puf* operon opposite to the direction of the *lac* promoter, pUI904. The *Eco*RI site in the polylinker of pUI904 was cleaved, and the linearized plasmid was partially digested with *Kpn*I. The 3.2-kb *Kpn*I-*Eco*RI fragment from pUI904 was isolated and inserted between the *Kpn*I and *Eco*RI sites of pUI900, and the structure of this plasmid, pUI902, was confirmed by restriction analysis (data not shown). The *Pst*I fragment from pUI902 was isolated and cloned into the *Pst*I site of pRK404 to yield pUI910, which contains the terminator-deleted *puf* operon in the opposite orientation with respect to the *lac* promoter.

Southern hybridization analysis of genomic DNA. Radioac-

tively labeled restriction fragment probes were prepared for Southern hybridization analysis as described previously by using [α-^{32}P]dCTP (14). Southern blots were performed by using the capillary transfer method (9) as described by Donohue et al. (14).

RNA isolation and quantitation. Total RNA was extracted from 600-ml cultures of mid-exponential-phase (cell density, 6×10^8 cells per ml) photosynthetically growing (100 W/m^2) *R. sphaeroides* as previously described (52), except that rifampin was added to the cultures to a final concentration of 50 μg/ml to prevent transcription initiations during isolation. For mRNA half-life determinations, rifampin was added to the cultures at a final concentration of 200 μg/ml. Portions (25 ml) were removed at various time intervals and processed for total RNA (21, 53). RNA was quantitated by the method of Mejbaum (32).

Northern (RNA) hybridization analysis. Strand-specific, ^{32}P-labeled RNA probes were synthesized from linearized and purified pBS plasmids (Table 1) in an in vitro transcription assay as specified by the manufacturer (Stratagene Inc., La Jolla, Calif.). Following transcription, the DNA templates were removed by treatment with 5 U of RQ_1 DNase (Promega Biotec, Madison, Wis.). Unincorporated [α-^{32}P]CTP was separated from the labeled fragments by using a spun column (28).

Analysis of mRNA by Northern (RNA) hybridization was performed by using 2 μg of total RNA which was denatured with glyoxal (42), separated on a 1.0% agarose gel (10.0 mM recirculating phosphate buffer [pH 7.0]), and transferred onto a nylon membrane (Nytran Modified Nylon-66; pore site, 0.45 μm; Schleicher & Schuell, Inc., Keene, N.H.) with an electroblot apparatus (Polyblot; American Bionetics Inc., Hayward, Calif.) as specified by the manufacturer. Approximate sizes of the mRNAs were estimated by using ethidium bromide-stained RNA ladders (Bethesda Research Laboratories Life Technologies, Inc., Gaithersburg, Md.) which had been treated as above. For quantitation, the area of the membrane filters corresponding to hybridized mRNA was excised and counted for radioactivity as previously described (52).

RNA half-life measurements were performed by denaturing 50 ng of RNA with formaldehyde as described (46), except that 0.1 M sodium phosphate (pH 6.8) was used as the buffer, and the RNA was transferred to nylon membranes (Nytran; Schleicher & Schuell) by using a slot format blotting apparatus (Bio-Dot Slot Format; Bio-Rad Laboratories, Richmond, Calif.) as specified by the manufacturers. Quantitation of hybridized [α-^{32}P]CTP-labeled strand-specific RNA probe was determined by scintillation counting as described above.

Low-temperature absorption spectral analysis. Low-temperature absorption spectra of membrane fractions from photosynthetically grown *R. sphaeroides* strains were recorded as previously described (19). The amount of functional RC was measured as described (37) in 20 mM 3-(*N*-morpholino)propanesulfonic acid (MOPS)–100 mM KCl (pH 7.0), with 10 μM valinomycin and 5 μM 2-undecyl-3-hydroxy-1,4-naphthoquinone. The E_h was adjusted to ca. 150 mV by the addition of sodium ascorbate. An extinction coefficient of 29.8 mM^{-1} cm^{-1} was used for quantitation of RC (15).

Cell fractionation and Western immunoblot analysis. Membrane and soluble fractions were prepared from exponentially grown photosynthetic cells by the methods of Chory et al. (7). Electrophoresis and transfer of the B875-α polypeptides were performed as previously described (23). Similar conditions were used for the RC-M and RC-H polypeptides, except that these proteins were transferred from the polyacrylamide gels to nitrocellulose filters (pore size, 0.45 μm) by electrophoresis at 40 V for 1 h in 25 mM sodium phosphate (pH 7.3)–10% (vol/vol) methanol (J. K. Wright, personal communication). All filters were treated to block nonspecific hybridizations by using the method of Batteiger et al. (3) as modified by Wright and Overath (49), with a final concentration of 1% (wt/vol) bovine serum albumin. The filters were treated with specific antibodies and detected with ^{125}I-labeled protein A as previously described (5). Quantitation was performed by gamma counting in a Gamma Trac Model 1193 (Tm Analytic, Elk Grove Village, Ill.). Immunoglobulin fractions of the B875-α antibody were prepared from sera as described (5). Immunoglobulin G antibodies were purified over an equal bed volume of anion exchange resin (DE52; Whatman, Inc., Clifton, N.J.) and eluted with 20 mM sodium phosphate (pH 7.0). *Staphylococcus aureus* protein A (Sigma Chemical Co., St. Louis, Mo.) was labeled with Na^{125}I by the method of Klinman and Howard (24).

Protein determination. The protein content was determined by the method of Lowry et al. (26) as modified by Markwell et al. (30). Bovine serum albumin was used as the standard.

Materials. Restriction endonucleases and nucleic acid-modifying enzymes were purchased from Bethesda Research Laboratories Life Technologies, Inc. or New England BioLabs, Inc., Beverly, Mass., and were used as specified by the manufacturers. The Klenow fragment of DNA polymerase, proteinase K, and X-Gal were obtained from Boehringer-Mannheim Biochemicals. [α-^{32}P]dCTP (800 Ci/mmol) and [α-^{32}P]CTP (400 Ci/mmol) were obtained from Amersham Corp., Arlington Heights, Ill. Carrier-free, reductant-free Na^{125}I (17 Ci/mg) was purchased from Du Pont, NEN Research Products, Boston, Mass. Nitrocellulose used for Southern hybridization analysis and Nytran membranes used for Northern hybridization analysis were from Schleicher & Schuell, Inc. IPTG and bovine serum albumin were obtained from Sigma. Glyoxal and X-Omat AR diagnostic X-ray film were the products of Eastman Kodak Co., Rochester, N.Y. With the exception of phenol (J. T. Baker Chemical Co., Phillipsburg, N.J.), which was distilled before use, all chemicals were of reagent grade purity and were used without further purification.

RESULTS

Recombination of a plasmid-encoded *puf* operon with the *R. sphaeroides* chromosome. We devised a strategy to insert the terminator-deleted *puf* operon (see below) into the chromosome of *R. sphaeroides* based on the following observations. The wild-type 4.5-kb *Pst*I restriction fragment (this fragment was previously determined to be 4.3 kb from restriction fragment mapping [10] but has now been more accurately sized following DNA sequence determinations) encompassing the entire *puf* operon (Fig. 2), as well as 5′-proximal and 3′-distal sequences, was cloned with the direction of the operon in the same (pUI581) and opposite (pUI580) orientations relative to the *lac* promoter of the RK2 derivative pRK404. These plasmids were conjugated from the mobilizing strain *E. coli* S17-1 into *R. sphaeroides* PUFB1 (10). PUFB1 contains a Km^r gene cartridge inserted within the ORF *Q* structural gene (W. A. Havelka, J. K. Lee, and S. Kaplan, manuscript in preparation) and extending into the *pufB* gene (Fig. 2) (10). PUFB1 does not produce *puf*-specific

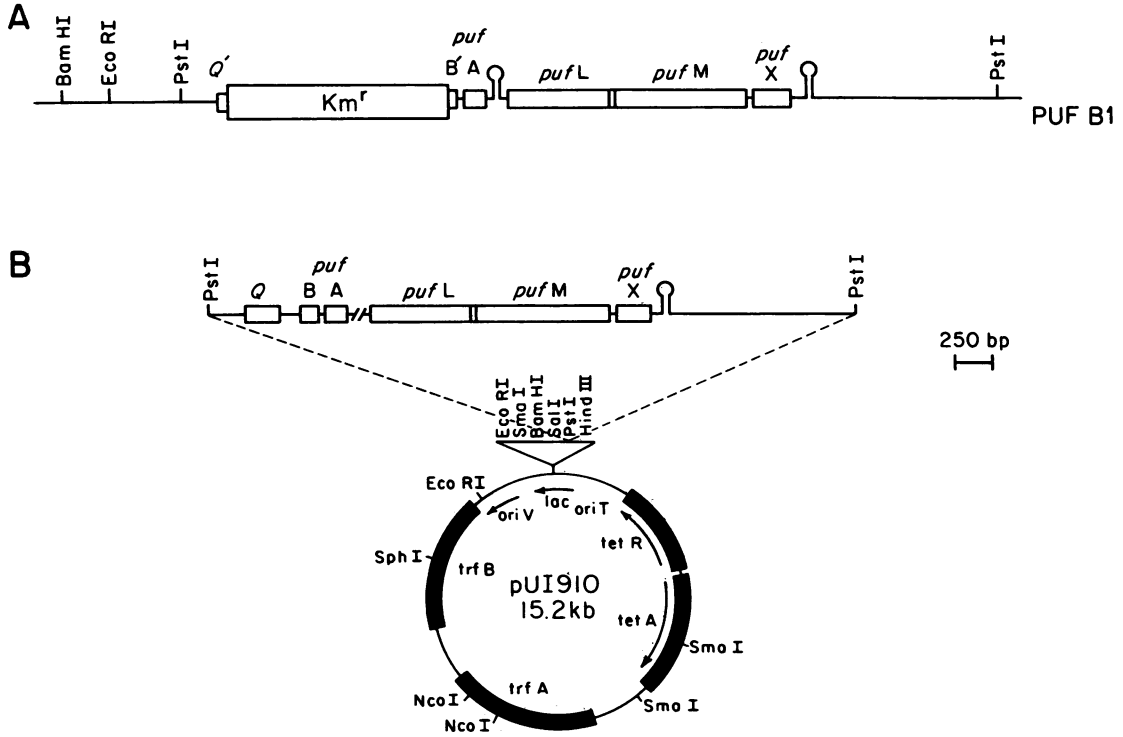

FIG. 2. Scheme for introducing site-specific mutations into the chromosomal copy of the *puf* operon. (A) Structure of the *puf* operon in PUFB1. Note the presence of the kanamycin resistance (Km^r) gene cartridge located between the *Acc*I site of ORF *Q* and the *Acc*I site of *pufB* (10). (B) Construction of pUI910, by insertion of an approximately 4,427-bp terminator-deleted *Pst*I fragment in the opposite orientation to that of the *lac* promoter into the *Pst*I site of pRK404 (see Materials and Methods for details). PUFB1 does not grow photosynthetically with pUI910 in *trans*. Strain PUFΔ348-420 was constructed by selecting colonies for photosynthetic growth as a result of an even-numbered reciprocal recombination between the 4,427-bp *Pst*I fragment of pUI910 and the chromosome of PUFB1.

transcripts, is photosynthetically incompetent, and is Km^r. A total of 100 Tc^r Km^r colonies were replica plated in the presence of tetracycline and kanamycin and incubated either aerobically or photosynthetically (10 W/m^2) at 32°C. All colonies of PUFB1(pUI581) grew both aerobically and photosynthetically at the same rate as the wild type. Although the 100 colonies of PUFB1(pUI580) grew aerobically as well as the wild type, no PUFB1(pUI580) colonies grew photosynthetically. Since the photosynthetic complementation of PUFB1 with the wild-type 4.5-kb *Pst*I fragment was orientation dependent, we concluded that a promoter for an essential gene was not present on this clone and that expression of this gene occurred only when the insert was downstream and presumably being driven from either the *lac* or *tet* promoter of pRK404. We know, by using purified RNA polymerase from *R. sphaeroides* in runoff transcription assays, that the promoter for the *Q* gene lies proximal to the *Pst*I restriction site 5′ to *Q* (J. Kansy and S. Kaplan, submitted for publication).

Thus, we used this information to select for the exchange of the PUFB1 genomic DNA, through homologous recombination, with the *puf* operon DNA located on the *Pst*I fragment and containing the terminator-deletion (see below). We anticipated that such a recombinant would be photosynthetically competent because genes *R* (immediately proximal to *Q*) and *Q* and the *puf* operon would all be *cis* to one another and the absence of B875 complexes does not limit photosynthetic growth in *R. sphaeroides* (18, 31).

Deletion of the intercistronic *puf* stem-loops. The intercistronic portion of the *puf* operon contains two regions of dyad symmetry capable of forming stable stem-loop structures, the first of which resembles a *rho*-independent transcription terminator (Fig. 1) (53). This putative terminator meets the two requirements for a *rho*-independent transcription terminator: a G+C-rich region of dyad symmetry forming a stem-loop structure and uracil residues following the hairpin structure. Only two U residues follow this terminator, perhaps because the DNA from *R. sphaeroides* is G+C rich. These stem-loops were deleted as described in Materials and Methods (Fig. 1A). The resulting intercistronic region is capable of forming an imperfect RNA secondary structure that does not resemble a *rho*-independent transcription terminator and is relatively unstable (Fig. 1B).

Construction of the terminator-deleted *puf* operon strain PUFΔ348-420. The *Pst*I fragment containing the terminator-deleted *puf* operon cloned into pRK404, i.e., pUI910, does not complement PUFB1 to photosynthetic competence. Therefore, we were able to select for a reciprocal recombination event between the *R. sphaeroides* DNA of pUI910 and the chromosome of PUFB1 by restored photosynthetic competence (Fig. 2). PUFB1(pUI910), which is unable to grow photosynthetically, was grown aerobically to late log phase. Cells (200 μl) were inoculated into 18 ml of fresh SSM supplemented with tetracycline and grown photosynthetically under illumination of 10 W/m^2. Following a 3-day lag, growth was apparent, and cells were plated on nonselective SSM. The resulting colonies were replica plated on nonselective SSM through two consecutive cycles of colony isolation to facilitate loss of the plasmid vector from the cells. The Km^s Tc^s colonies were identified and further streak purified. The crossovers must have occurred both upstream and downstream of the Km^r gene cartridge so that

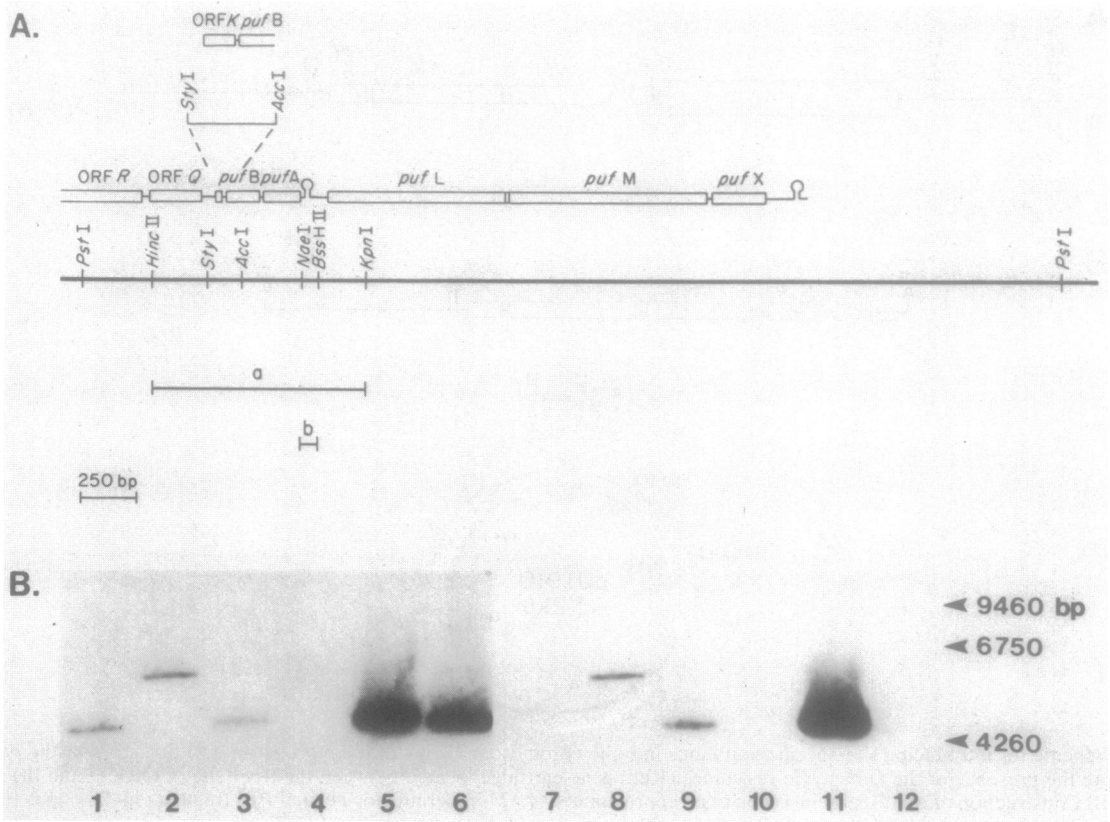

FIG. 3. Southern hybridization analysis of the terminator-deleted *puf* operon in strain PUFΔ348-420. (A) Restriction endonuclease map of the DNA encompassing the *puf* operon and the two DNA fragments (a and b) used as probes for the hybridizations. (B) Autoradiograms of a Southern hybridization blot confirming the 73-bp *Nae*I-*Bss*HII deletion from the intercistronic region of the *puf* operon in strain PUFΔ348-420. Lanes: 1 and 7, total chromosomal DNA from PUFΔ348-420; 2 and 8, total chromosomal DNA from PUFB1; 3 and 9, total chromosomal DNA from 2.4.1; 4 and 10, linearized DNA from λ *c*I *ts*857; 5 and 11, linearized DNA from pUI580; 6 and 12, linearized DNA from pUI902. The DNA from PUFΔ348-420, PUFB1, 2.4.1, pUI580, and pUI902 were digested with *Pst*I, and the DNA from λ *c*I *ts*857 was digested with *Hin*dIII, separated on 1.0% agarose gels, and transferred to nitrocellulose by capillary action. DNA from pUI580 and pUI902 was used as controls with the wild-type and the terminator-deleted *puf* operon, respectively. *Hin*dIII digests of λ *c*I *ts*857 served as molecular weight standards and as negative controls for the hybridizations. Lanes 1 to 6 were probed with the 986-bp *Hinc*II-*Kpn*I restriction fragment (panel A, probe a) isolated from pUI710. Lanes 7 to 12 were probed with the 73-bp *Nae*I-*Bss*HII restriction fragment (panel A, probe b) isolated from pUI710.

the entire ORF *Q* and *pufB* reading frames would be reestablished and the Km^r cartridge on the chromosome would be lost. Thus, through the use of appropriate selective conditions, we have been able to introduce specific gene alterations into the chromosome of *R. sphaeroides*.

Southern hybridization analysis confirmed the construction (Fig. 3). The data in Fig. 3 proved that the 73-bp *Nae*I-*Bss*HII fragment was deleted from the intercistronic region of the *puf* operon in PUFΔ348-420, probably as a result of a reciprocal recombination between the terminator-deleted *puf* operon and the Km^r gene plus downstream *puf* DNA of PUFB1. The approximately 4,427-bp *puf*-specific *Pst*I fragment of PUFΔ348-420 appears to migrate slightly ahead of the 4,500-bp *Pst*I fragment of the wild type on a 1.0% agarose gel, indicative of a small deletion (Fig. 3B, lanes 1 and 3), but by itself cannot constitute evidence of the deletion. Figure 3B also reveals the chromosomal replacement of the 5,630-bp *Pst*I fragment of PUFB1 chromosomal DNA (lane 2) with the 4,427-bp *Pst*I fragment of the terminator-deleted operon (lane 1). An identical blot was probed with the 73-bp deleted *Nae*I-*Bss*HII fragment (Fig. 3B, lanes 7 to 12). As expected, DNA from PUFΔ348-420 and the control, pUI903, did not hybridize with this fragment. The probe hybridized to DNA from PUFB1, 2.4.1, and the positive control, pUI580. Probes from either the Km^r gene or pRK404 did not hybridize to PUFΔ348-420 DNA, demonstrating that the plasmid product of the recombination event was lost from this strain (data not shown).

Low-temperature spectral analysis of PUFΔ348-420. Figure 4 shows the low-temperature absorption spectra obtained from the membrane fractions of strains RS103 (18, 23, 31), 2.4.1, and PUFΔ348-420 grown at 100 W/m^2 and measured at 77 K, as described in Materials and Methods. Measurements were performed at low temperature because the B875 spectral complex of PUFΔ348-420 could not be detected at 300 K. RS103 was used as a negative control, since it lacks the characteristic B875 spectral peak (18, 23, 31). PUFΔ348-420 contains approximately 7% of the wild-type level of B875 spectral complex that appears as a shoulder on the near-infrared side of the B850 peak, whereas the amount of functional RC in PUFΔ348-420 was only 25% that of wild type (Table 2). The amount of the B800-850 spectral complex in the mutant was increased approximately twofold over that of the wild type, which is also true for strain RS103.

The differences in the relative amounts of spectral complexes and functional RC may account for the decreased

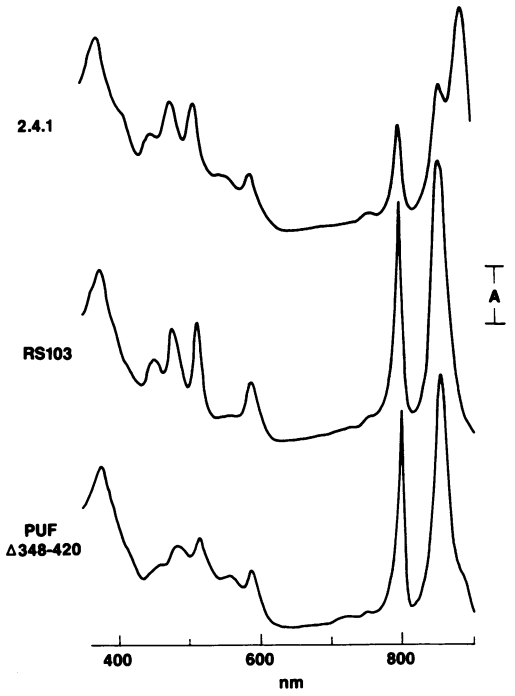

FIG. 4. Low-temperature spectral analysis of 2.4.1, PUFΔ348-420, and RS103 grown at 100 W/m^2, measured near 77 K. RS103 was used as a negative control for the B875 spectral complex (18). The B875 shoulder of PUFΔ348-420 is resolved at this temperature. The relative amounts of the B875 and B800-850 spectral complexes are presented in Table 2. The relative amounts of functional RC, measured spectrally as described (37), are also presented.

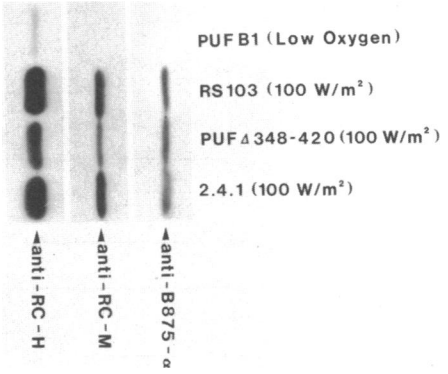

FIG. 5. Western immunoblot analysis with antibodies raised against B875-α, RC-M, and RC-H; ^{125}I-labeled protein A was used for detection. A 5-μg portion of membrane fractions was analyzed from photoheterotrophically grown RS103, PUFΔ348-420, and 2.4.1 and low-oxygen-grown PUFB1. PUFB1 served as a negative control for B875-α and RC-M polypeptides. Previously, the relative amount of B875-α in RS103 was compared with that in the wild type (23). The soluble fractions from each strain were analyzed, and no significant amounts of polypeptides were detected (data not shown). The radiolabeled filters were cut out and quantitated by gamma emission. The relative amounts of each polypeptide are presented in Table 2.

growth rates of the mutant cultures when illuminated with decreased light intensities. At an incident light intensity of 100 W/m^2, strains 2.4.1 and PUFΔ348-420 had similar doubling times of 2.5 and 2.7 h, respectively. However, when the light intensity was lowered to 10 W/m^2, strain 2.4.1 doubled in 3.0 h, whereas PUFΔ348-420 doubled in 4.7 h. When we reduced the incident light intensity to 3 W/m^2, strain 2.4.1 doubled in 10 h, whereas the doubling time of PUFΔ348-420 was approximately 17.5 h. The lower growth rates of PUFΔ348-420 at lowered light intensities is presumably due to the inability of the photosynthetic unit to carry out optimal photochemistry. However, it is evident that a substantially altered photosynthetic unit size need have very little effect on cell growth at either medium or high light intensities, under laboratory conditions.

Western immunoblot analysis. Studies with mutant RS103 show that the absence of the B875 spectral complex does not necessarily indicate the absence of the B875 polypeptides (18, 23, 31). Therefore, we examined the amount of B875-α and RC-M and RC-H polypeptides by Western immunoblot analysis (Fig. 5). Membrane proteins from photosynthetically grown RS103, PUFΔ348-420, and 2.4.1 (incident light intensity, 100 W/m^2) and low-oxygen-grown PUFB1 cells were separated by sodium dodecyl sulfate-polyacrylamide gel electrophoresis, transferred to nitrocellulose, and reacted individually with B875-α-, RC-M-, and RC-H-specific antibodies, as described in Materials and Methods. Cells were grown at 100 W/m^2, since their generation times are essentially equal at this light intensity. PUFB1, grown in the presence of a low oxygen tension, was used as a negative control for the B875-α and RC-M polypeptides. A summary of the relative amounts of each polypeptide detected in each strain is presented in Table 2. The amount of B875-α polypeptide in PUFΔ348-420 was approximately 56% of the wild type, whereas the amount of RC-M was 58% of that found in the wild type. RC-H was present in PUFΔ348-420 at 65% of the wild-type level. Titration of the membrane

TABLE 2. Relative amounts of spectral complexes, functional RC, and cellular levels of B875-α, RC-M, and RC-H polypeptides from cells grown at 100 W/m^2

Strain	Relative amt of following spectral complexes[a] and functional RC[b]:			Relative amt of following membrane polypeptide[c]:		
	B875	B800-850	RC	B875-α	RC-M	RC-H
2.4.1	100	100	100	100	100	100
PUFΔ348-420	7	192	25	56	58	65
RS103	0	290	89	31	96	102
PUFB1[d,e]	0	25	0	0	0	20

[a] Levels of spectral complexes were measured at 77 K and standardized to those of the wild type.
[b] Levels of functional RC were measured as described (37).
[c] Levels of antigenic proteins were normalized with respect to those of the wild type.
[d] Photosynthetically incompetent PUFB1 cells were grown at low oxygen tension.
[e] Levels of spectral complexes and functional RC in PUFB1 were determined previously at 300 K (10).

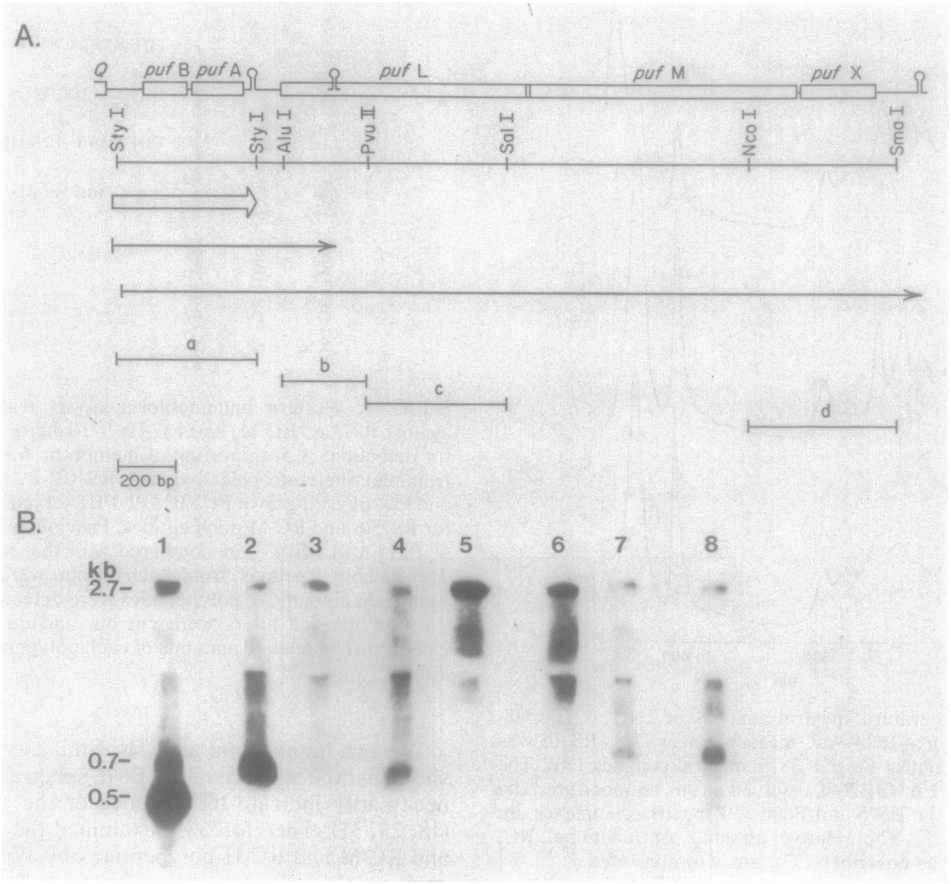

FIG. 6. Analysis of *puf* operon mRNA from the wild type and PUFΔ348-420 grown photosynthetically at a light intensity of 100 W/m^2. (A) Restriction endonuclease map of the *puf* operon, a representation of the three *puf*-specific mRNAs, and the location of the four *puf*-specific RNA probes a, b, c, and d. (B) Northern hybridization analyses with [α-^{32}P]CTP-labeled RNA probes. RNA from the wild type (lanes 1, 3, 5, and 7) and PUFΔ348-420 (lanes 2, 4, 6, and 8) were hybridized with RNA probes a (lanes 1 and 2), b (lanes 3 and 4), c (lanes 5 and 6), and d (lanes 7 and 8). The RNA probes a, b, c, and d were generated by in vitro transcription of pUI655, pUI662, pUI658, and pUI663, respectively.

fractions with respect to total membrane protein loaded ensured that the amount of protein loaded per lane and its detection by each specific antibody were within the linear range of the assay. Using a similar method, we were unable to detect any of these polypeptides in the soluble fractions derived from extracts of these strains when probed with each of the three antibodies (data not shown). The level of B875-α polypeptide in RS103 agreed well with previous determinations (23).

In vivo expression of the *puf* operon. The absence of the *pufAL* intercistronic stem-loops would be expected to lead to the loss of the 0.5-kb transcript, since all of the transcripts would extend through the *pufAL* region. Total RNA from *R. sphaeroides* 2.4.1 and the mutant PUFΔ348-420 was isolated from cells grown photosynthetically at 100 W/m^2 as described in Materials and Methods, and Northern hybridization analysis was performed to identify the *puf*-specific transcripts in each strain (Fig. 6). RNA from each strain was hybridized with four strand-specific RNA probes (Fig. 6A, probes a, b, c, and d). Three transcripts of approximately 0.5, 0.7, and 2.7 kb were identified from the 2.4.1 RNA (Fig. 6B, lane 1). Lanes 1 and 2 are overexposed, and so we can conclude that no 0.5-kb transcript was present in the terminator-deleted strain. Previously, we had used DNA probes and GeneScreen filters (52) and were able to identify only the 2.7- and 0.5-kb transcripts. The use of Nytran filters with increased RNA-binding capacity and high-activity RNA probes permitted us to identify the 0.7-kb transcript. However, the use of these conditions increased the levels of background binding to the rRNA seen in the region of the middle of each of the lanes and independent of the probe used. RNA probes b and c were used to localize the 3′ end of the 0.7-kb transcript from 2.4.1. RNA probe b hybridized to the 0.7- and 2.7-kb transcripts but not the 0.5-kb mRNA (Fig. 6B, lane 3). Only the 2.7-kb transcript was detected with RNA probe c (Fig. 6B, lane 5). Therefore, the 3′ end of the 0.7-kb mRNA in 2.4.1 cells must map to a location within the proximal region of the *pufL* structural gene. We have recently analyzed the 3′ and 5′ ends of each transcript in both wild-type and PUFΔ348-420 strains by S1 nuclease mapping (Lee et al., in preparation), and the arrows in Fig. 6A are drawn to correspond to the approximate ends of each transcript.

The effects on the existence of each of the three *puf* messages were analyzed following deletion of the intercistronic stem-loops. Two transcripts of approximately 0.63 and 2.63 kb from strain PUFΔ348-420 were detected with RNA probe b (Fig. 6B, lane 4), and only the 2.63-kb transcript was detected with RNA probe c (lane 6). These transcripts correspond to the sizes of the large (2.7-kb) and the medium

TABLE 3. Relative levels and half-lives of *puf*-specific mRNA transcripts for 2.4.1 and PUFΔ348-420[a]

Transcript	Size (kb)	Strain	Relative amt[b]	$t_{\frac{1}{2}}$ (min)
Large	2.7	Wild type	7.6	8
	2.63	PUFΔ348-420	4.5	3
Medium	0.7	Wild type	2.3	14
	0.63	PUFΔ348-420	5.1	6
Small	0.5	Wild type	100.0	21
	ND[c]	PUFΔ348-420	ND	ND

[a] The strains were grown photosynthetically at 100 W/m^2.
[b] Levels of *puf*-specific transcripts were normalized to the amount of 0.5-kb mRNA in the wild type, which is arbitrarily set at a value of 100. Data were obtained by using the *pufBA*-specific RNA probe.
[c] ND, Not detected.

(0.7-kb) transcripts in 2.4.1 minus the 73-bp deletion in the *puf* operon created in PUFΔ348-420. Since the 0.63-kb transcript was not detected with RNA probe c (Fig. 6B, lane 6), we are led to conclude that the 0.63-kb transcript terminates within the proximal region of the *pufL* structural gene, as does the 0.7-kb mRNA in strain 2.4.1. The relative amounts of each transcript are presented in Table 3. Note that several Northern blots in Fig. 6 are heavily exposed. This was done deliberately to clearly demonstrate that a transcript was not present when indicated. All of these experiments were repeated several times, with identical results. From these data, we conclude that the level of the PUFΔ348-420 0.64-kb transcript increased approximately 2.5-fold over wild-type levels but the level of the 2.63-kb transcript decreased by nearly 40%. Additionally, smaller breakdown products were detected with the 3′-most RNA probe, probe d (Fig. 6B, lanes 7 and 8), than those observed with the b and c probes (Fig. 6B, lanes 3 to 6), although probe c (lanes 5 and 6), corresponding to an internal segment of the *L* gene, revealed considerable breakdown products.

Determination of mRNA stability. We had shown previously (53), as well as here, that the large *puf* transcript appears to decay as the result of 5′-localized endonucleolytic cleavage(s). We might expect that the large transcript in the terminator-deletion strain possesses an altered half-life owing to the absence of substantial secondary structures that could block exonucleases. The decay of each *puf*-specific mRNA was determined in photosynthetically grown *R. sphaeroides* 2.4.1 and PUFΔ348-420 (Fig. 7). The decay rates of the wild-type 0.5-kb transcript and the terminator-deleted 0.63-kb transcript were determined by slot blot transfer and hybridization with the *pufBA*-specific probe (Fig. 6A, probe a). The half-lives of the large (2.7- and 2.63-kb) transcripts of these strains were also determined by slot blot transfer, except that the *pufL*-specific probe (Fig. 6A, probe c) was used. The half-life of the wild-type 0.7-kb transcript was determined by Northern hybridization analysis with the *pufBA*-specific probe. The amount of RNA transferred per slot and its detection were within the linear range of the assays. These decay values were identical to those obtained by Northern hybridization analysis (data not shown). The half-life for each transcript is presented in Table 3. The stability of the 2.7-kb transcript in the wild type decreased to approximately 33% of its original value when the intercistronic stem-loops were deleted, whereas the stability of the 0.63-kb transcript decreased to approximately 40% of the value determined for the 0.7-kb transcript. Thus, deletion of the intercistronic stem-loops had a significant

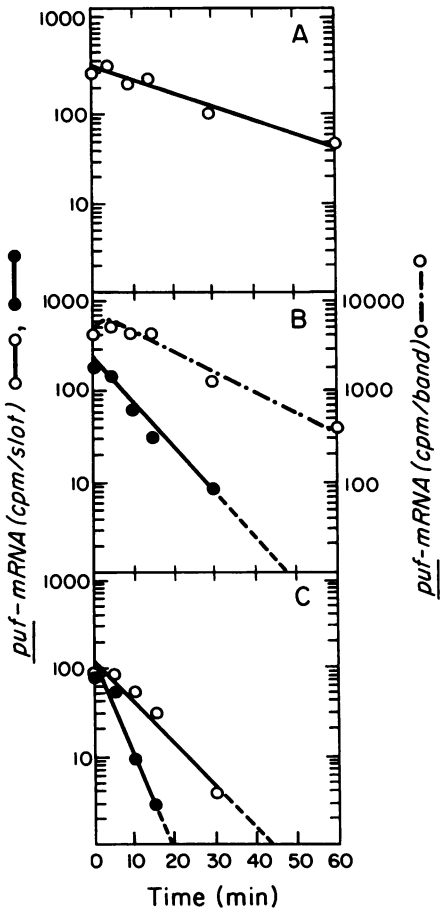

FIG. 7. Stability of *puf*-specific mRNAs in the wild type and PUFΔ348-420 grown at a light intensity of 100 W/m^2. The amounts of *puf*-specific mRNAs from the wild type (○) and from PUFΔ348-420 (●) after the addition of rifampin are shown on semilogarithmic plots: panel A, the 0.5-kb transcript; panel B, the 0.7-kb (0.63-kb) transcripts; panel C, the 2.7-kb (2.63-kb) transcripts. The amounts of *puf*-specific mRNAs present were determined by slot blot (——) or by Northern hybridization (—·—·—) analysis as described in Materials and Methods. The 0.5- and 0.7-kb (0.63-kb) transcripts were hybridized with the [α-^{32}P]CTP-labeled *pufBA*-specific RNA probe (Fig. 6A, probe a). The 2.7-kb (2.63-kb) transcripts were hybridized with the [α-^{32}P]CTP-labeled *pufL*-specific RNA probe (Fig. 6A, probe c). The amount of probe hybridized was determined by scintillation counting. The half-lives of the transcripts are presented in Table 3.

effect on the stability of *puf* operon mRNA both 5′ and 3′ of this region.

DISCUSSION

We have constructed a strain of *R. sphaeroides* (PUFΔ348-420) in which the putative intercistronic terminator believed to give rise to the small transcript of the *puf* operon has been deleted from the chromosome. We chose to construct PUFΔ348-420 instead of using a *puf*-deleted strain complemented in *trans* with the terminator-deleted *puf* operon to exclude the possibility of interfering with possible *cis*-acting arrangements of the DNA upstream of the *puf* operon and of introducing spurious copy number effects. As an example of the difficulties which can be encountered, the deletion of stem-loop structures from the intercistronic re-

gion of the *malEFG* operon of *E. coli* in a plasmid-encoded operon reduced the level of *malE* protein by only two- to threefold, whereas the identical deletion from the chromosome reduced *malE* expression by approximately ninefold (35). When more mRNA is transcribed from multicopy plasmids than from the chromosome, *trans*-regulatory factors, should they exist, may become limiting. A previous study by Davis et al. (10) has shown that pRK404 derivatives containing fragments of the *puf* operon supplied in *trans* in PUFB1 exist in four to six copies per cell. In addition, we have observed that the level of *puf* operon-specific transcripts produced in *trans* in PUFB1(pUI581) was approximately fourfold higher than the amount detected in the wild type (B. S. DeHoff and S. Kaplan, unpublished data).

Our studies showed that the generation time of the mutant was identical to that of the wild type at 100 W/m^2, whereas at low light intensity (3 W/m^2) the generation time was approximately twofold longer, presumably due to inefficient transfer of excitation energy from the spectral complexes to the RC. Because RS103, which lacks B875 complexes, does not grow at 3 W/m^2, we conclude that the B875 complex is obligatory for excitation transfer from the B800-850 complex to the RC.

At 100 W/m^2 the relative amounts of B875-α, RC-M, and RC-H polypeptides in the mutant were approximately 56, 58, and 65%, respectively, of those in the wild type. The reduction of B875-α and RC-M polypeptides correlates directly with the decreased abundance in the steady-state levels of the *puf*-specific mRNAs. However, the amount of RC-H polypeptide decreased, even though the level of *puhA* mRNA, which encodes RC-H (13), increased twofold (DeHoff and Kaplan, unpublished). Low-temperature spectral analysis revealed approximately 7% of the B875 spectral complex in PUFΔ348-420 relative to the wild type. The amount of B800-850 spectral complexes has increased approximately twofold over that of the wild type; this correlates well with the twofold increase of *puc* mRNA (DeHoff and Kaplan, unpublished), which encodes the B800-850 polypeptides (21). Additionally, the amount of intact RC determined spectrally was 25% of the wild type. If the ratio of B875 to RC is approximately 15:1 in the wild type (1), this ratio must be approximately 4:1 in PUFΔ348-420. Obviously, there are other requirements for proper assembly of the B875 and RC spectral complexes which extend beyond the abundance of either the RNA, the apopolypeptides, or the cellular level of bacteriochlorophyll. Additionally, analyses such as these point out the interrelationships between the *puhA*, *puf*, and *puc* operons at both the transcriptional and posttranscriptional levels.

The removal of a putative transcription terminator from the intercistronic region of the *puf* operon should allow RNA polymerase to read through this region to produce an increased level of downstream RNA and a concomitant disappearance of the shorter transcript. We have compared the abundance of the *puf* operon-specific transcripts in the terminator-deleted strain, PUFΔ348-420, with that of transcripts in the wild-type strain, 2.4.1. The 0.5-kb *puf* transcript is absent in PUFΔ348-420, whereas the abundance of the 0.63-kb mRNA, which corresponds to the 0.7-kb mRNA of the wild type with 73 bases deleted, increased by approximately 2.5-fold. The increased abundance of the 0.63-kb transcript must result from readthrough of the intercistronic region by the RNA polymerase and not from degradation of the 3′ end of the 2.7-kb transcript of the operon. If the abundance of the 0.63-kb transcript resulted solely from 3′ degradation, one would expect at least as much of this transcript in the wild type, since the 3′ end of the operon is identical in the construct and wild-type strains. Additionally, the transcription initiation site of the 0.63-kb mRNA appears to be identical to that of the wild-type 0.5-kb transcript (Lee et al., in preparation). Furthermore, if we consider the decreased half-lives of the large and medium transcripts in the terminator-deletion strain, which are approximately 33 and 40% of the wild-type half-lives, respectively, then we estimate, from the steady-state levels of these transcripts, that transcription through the *pufAL* terminator region has increased at least 10-fold in the mutant strain. This value is close to that predicted from the measured ratio of 0.5-, 0.7-, and 2.7-kb transcripts in the wild type. These data support the hypothesis that the first stem-loop within the intercistronic region of the *puf* operon functions as a transcription terminator in vivo.

Klug et al. (25) have reported the transcriptional consequences in *R. capsulatus* arising from deletion of the stem-loop structure from the intercistronic region of the *puf* operon in a construct provided in *trans* in a strain with a chromosomal deletion of the *puf* operon. They detected equivalent amounts of the large transcript in strains containing both the altered and the unaltered copies of the *puf* operon. They detected no small transcript in strains containing the altered copy. These workers suggest that the stem-loop structure functions to protect RNA from 3′ exoribonucleolytic digestion rather than to terminate transcription. However, a direct assay for protection against 3′ exoribonucleolytic digestion in vivo did not detect any protective effect (6). We also measured the abundances of the large transcript of 2.7 kb compared with total cellular RNA for *R. sphaeroides* PUFΔ348-420 and 2.4.1. In contrast to the finding for *R. capsulatus*, the abundance of the large mRNA in the terminator-deleted strain was only 60% of that in the wild type. Additionally, the large *puf* transcript was destabilized by removal of the intercistronic stem-loops which are 5′ of the *pufLMX* region, even though the 3′ ends of these mRNAs are unaltered. It is apparent from our results for *R. sphaeroides* that the intercistronic region, which is capable of forming the stem-loop structures, is required for stabilizing the intact *puf*-specific mRNAs and thereby contributes to maintaining the proper balance of *puf* transcripts. We conclude that the factors which govern mRNA stability are complex. However, the intercistronic stem-loop structures are probably not potential processing sites, since their removal decreased, rather than increased, mRNA stability.

Can the differences observed between these studies with *R. sphaeroides* and those with *R. capsulatus* be reconciled? It is possible that these organisms use different mechanisms by which they regulate the cellular levels of the various spectral complexes. Recently, Chen et al. (6) have come to a similar conclusion with respect to a suspected transcription terminator within the *puc* operon of *R. capsulatus*, as we did earlier with regard to the intercistronic stem-loop structure followed by the sequence -AUUC- within the *puf* operon in *R. sphaeroides* (Fig. 1) (53) serving as a transcription terminator. A second possibility is that these species use identical regulatory mechanisms, and yet a third possibility is that the mechanisms, although similar, are less stringent in one species than the other. *R. capsulatus* produces spectral complexes even under conditions of high O_2 tension (16), whereas *R. sphaeroides* does not (7). It is possible that the analysis of the *R. capsulatus* data is compromised by (i) the use of multi-copy-number plasmids supplied in *trans*, (ii) the lack of sufficient upstream or downstream DNA sequences *cis* to the *puf* operon, and (iii) the use of semiaerobic

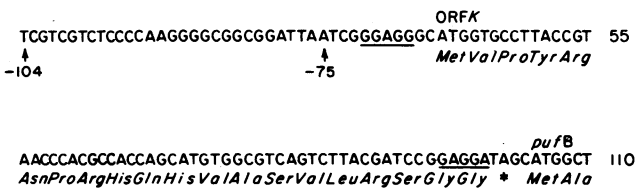

FIG. 8. DNA sequence encompassing a putative ORF *K*, immediately upstream of the *pufB* gene. The 20 amino acids encoded by ORF *K* are shown beneath the DNA sequence. Additionally, the first two amino acids encoded by the *pufB* structural gene are presented. The proposed Shine-Dalgarno sequences for both ORF *K* and *pufB* genes are underlined. The initiation sites for the 0.5- and 2.7-kb transcripts are indicated by arrows at positions −104 and −75, respectively, upstream of the start codon for the *pufB* structural gene.

cultures, which would be undergoing derepression of a complex and changing variety of mRNAs.

If the intercistronic stem-loop is a transcription terminator for the formation of the small *puf* operon transcript, how are the distal *pufLMX* genes transcribed? One possible model, proposed recently by Kiley and Kaplan (22) and refined here, suggests that the ORF containing 20 codons, 9 of which are rare, immediately upstream of *pufB*, namely, ORF *K*, influences stalling of the ribosomes (Fig. 8). The 5′ termini of the small and the large *puf* transcripts map at approximately −104 and −75 nucleotides, respectively, upstream of the *pufB* structural gene (53). We propose here that during the synthesis of the small and medium transcripts, ribosomes are able to attach to the Shine-Dalgarno sequence upstream of ORF *K* and stall during translation. Similar to attenuation (51), translation uncouples from transcription, and the RNA polymerase terminates very efficiently at the intercistronic region, producing the small transcript, because the secondary structure in the intercistronic region would form. Some readthrough does occur, and the RNA polymerase may terminate at the stem-loop structure within the proximal region of *pufL*. However, we suggest that during synthesis of the large transcript, ribosomes do not attach to the Shine-Dalgarno sequence upstream of ORF *K*, since it is too close to the 5′ end of that transcript (3 to 5 nucleotides), but do attach to the Shine-Dalgarno sequence immediately upstream of *pufB*. As a consequence, transcription and translation remain coupled, and RNA polymerase reads through the intercistronic stem-loops because the adjacent ribosomes prevent their formation; thus, termination does not take place. This mechanism would ensure strict regulation of the levels of *puf* mRNA in the cell. This hypothesis is supported by the observation that an in-frame fusion of ORF *K-pufB* gives rise to both the fused gene product and the unfused β-polypeptide (W. A. Havelka and S. Kaplan, unpublished results).

Thus, we believe that site-directed alterations in the stem structure of the intercistronic terminator will further alter the ratio of large and small transcripts derived from the *puf* operon, and, with such changes, alterations in the cellular levels of the spectral complexes are to be expected.

ACKNOWLEDGMENTS

We thank R. C. Prince, Exxon Research and Engineering Co., Annandale, N.J., for providing the low-temperature spectral data; P. J. Kiley and J. H. Hoger for preparation of sera for Western immunoblot analysis; T. N. Tai for constructing pUI580 and pUI581; and M. D. Moore for providing bacteriophage RS1 and assistance in preparation and photography of the figures. We also thank J. K. Wright for advice in purification of the B875-α antibody.

This work was supported by Public Health Service grants GM15590 and GM31667 to S.K. from the National Institutes of Health and by Department of Agriculture grant AG85-CRCR-1-1809 to S.K., T.J.D., and R.I.G.

LITERATURE CITED

1. **Aagaard, J., and W. R. Sistrom.** 1972. Control of synthesis of reaction center bacteriochlorophyll in photosynthetic bacteria. Photochem. Photobiol. **15**:209–225.
2. **Adhya, S., and M. Gottesman.** 1978. Control of transcription termination. Annu. Rev. Biochem. **47**:967–996.
3. **Batteiger, B., V. W. J. Newhall, and R. B. Jones.** 1982. The use of Tween-20 as a blocking agent in the immunological detection of proteins transferred to nitrocellulose membranes. J. Immunol. Methods **55**:297–307.
4. **Birnboim, H. C., and J. Doly.** 1979. A rapid alkaline extraction procedure for screening recombinant plasmid DNA. Nucleic Acids Res. **7**:1513–1523.
5. **Burnette, W. N.** 1981. "Western blotting": electrophoretic transfer of proteins for sodium dodecyl sulfate-polyacrylamide gels to unmodified nitrocellulose and radiographic detection with antibody and radioiodinated protein A. Anal. Biochem. **112**:195–203.
6. **Chen, C.-Y. A., J. T. Beatty, S. N. Cohen, and J. G. Belasco.** 1988. An intercistronic stem-loop structure functions as an mRNA decay terminator necessary but insufficient for *puf* mRNA stability. Cell **52**:609–619.
7. **Chory, J., T. J. Donohue, A. R. Varga, L. A. Staehelin, and S. Kaplan.** 1984. Induction of the photosynthetic membranes of *Rhodopseudomonas sphaeroides*: biochemical and morphological studies. J. Bacteriol. **159**:540–554.
8. **Cohen, S. N., A. C. Y. Chang, and L. Hsu.** 1972. Nonchromosomal antibiotic resistance in bacteria: genetic transformation of *E. coli* by R-factor DNA. Proc. Natl. Acad. Sci. USA **69**:2110–2114.
9. **Davis, R. W., D. Botstein, and J. R. Roth (ed.).** 1980. Advanced bacterial genetics: a manual for genetic engineering. Cold Spring Harbor Laboratory, Cold Spring Harbor, N.Y.
10. **Davis, J., T. J. Donohue, and S. Kaplan.** 1988. Construction, characterization, and complementation of a Puf⁻ mutant of *Rhodobacter sphaeroides*. J. Bacteriol. **170**:320–329.
11. **Ditta, G., T. Schimdhauser, E. Yakobson, P. Lu, X.-W. Liang, D. R. Finlay, D. Guiney, and D. R. Helinski.** 1985. Plasmids related to the broad host range vector, pRK290, useful for gene cloning and for monitoring gene expression. Plasmid **13**:149–153.
12. **Donohue, T. J., J. Chory, T. E. Goldsand, S. P. Lynn, and S. Kaplan.** 1985. Structure and physical map of *Rhodopseudomonas sphaeroides* bacteriophage RS1 DNA. J. Virol. **55**:147–157.
13. **Donohue, T. J., J. H. Hoger, and S. Kaplan.** 1986. Cloning and expression of the *Rhodobacter sphaeroides* reaction center H gene. J. Bacteriol. **168**:953–961.
14. **Donohue, T. J., A. G. McEwan, and S. Kaplan.** 1986. Cloning, DNA sequence, and expression of the *Rhodobacter sphaeroides* cytochrome c_2 gene. J. Bacteriol. **168**:962–972.
15. **Dutton, P. L., K. M. Petty, H. S. Bonner, and S. D. Morse.** 1975. Cytochrome c_2 and reaction center of *Rhodopseudomonas sphaeroides* Ga. membranes. Extinction coefficients, content, half-reduction potentials, kinetics and electric field alterations. Biochim. Biophys. Acta **387**:536–556.
16. **Garcia, A. F., G. Drews, and H. H. Reidl.** 1981. Comparative studies of two membrane fractions isolated from chemotrophically and phototrophically grown cells of *Rhodopseudomonas capsulata*. J. Bacteriol. **145**:1121–1128.
17. **Griffith, O. M.** 1986. Isolation of plasmid DNA from cleared lysates by the gradient relaxation method. Applications Data DS-675. Beckman Instruments, Inc., Spinco Division, Palo Alto, Calif.
18. **Jackson, W. J., P. J. Kiley, C. E. Haith, S. Kaplan, and R. C. Prince.** 1987. On the role of the light-harvesting B880 in the correct insertion of the reaction center of *Rhodobacter capsu-*

latus and *Rhodobacter sphaeroides*. FEBS Lett. **215**:171–174.
19. **Jackson, W. J., R. C. Prince, G. J. Stewart, and B. L. Marrs.** 1986. Energetic and topographic properties of a *Rhodopseudomonas capsulata* mutant deficient in the B870 complex. Biochemistry **25**:8440–8446.
20. **Kiley, P. J., T. J. Donohue, W. A. Havelka, and S. Kaplan.** 1987. DNA sequence and in vitro expression of the B875 light-harvesting polypeptides of *Rhodobacter sphaeroides*. J. Bacteriol. **169**:742–750.
21. **Kiley, P. J., and S. Kaplan.** 1987. Cloning, DNA sequence, and expression of the *Rhodobacter sphaeroides* light-harvesting B800-850-α and B800-850-β genes. J. Bacteriol. **169**:3268–3275.
22. **Kiley, P. J., and S. Kaplan.** 1988. Molecular genetics of photosynthetic membrane biosynthesis in *Rhodobacter sphaeroides*. Microbiol. Rev. **52**:50–69.
23. **Kiley, P. J., A. Varga, and S. Kaplan.** 1988. Physiological and structural analysis of light-harvesting mutants of *Rhodobacter sphaeroides*. J. Bacteriol. **170**:1103–1115.
24. **Klinman, D. M., and J. C. Howard.** 1980. Protein iodination suitable for labeling hybridoma antibodies, p. 401–402. *In* R. H. Kennett, T. J. McKearn, and K. B. Bechtol (ed.), Monoclonal antibodies. Plenum Publishing Corp., New York.
25. **Klug, G., C. W. Adams, J. G. Belasco, B. Doerge, and S. N. Cohen.** 1987. Biological consequences of segmental alterations in mRNA stability: effects of deletion of the intercistronic hairpin loop region of the *Rhodobacter capsulatus puf* operon. EMBO J. **6**:3515–3520.
26. **Lowry, O. H., N. J. Rosebrough, A. L. Farr, and R. J. Randall.** 1951. Protein measurement with the Folin phenol reagent. J. Biol. Chem. **193**:265–275.
27. **Leuking, D. R., R. T. Fraley, and S. Kaplan.** 1978. Intracytoplasmic membrane synthesis in synchronous cell populations of *Rhodopseudomonas sphaeroides*. J. Biol. Chem. **253**:451–457.
28. **Maniatis, T., E. F. Fritsch, and J. Sambrook.** 1982. Molecular cloning: a laboratory manual. Cold Spring Harbor Laboratory, Cold Spring Harbor, N.Y.
29. **Maquat, L. E., and W. S. Reznikoff.** 1978. In vitro analysis of the *Escherichia coli* RNA polymerase interaction with wild-type and mutant lactose promoters. J. Mol. Biol. **125**:467–490.
30. **Markwell, M. A., S. M. Haas, L. L. Bieber, and N. E. Tolbert.** 1978. A modification of the Lowry procedure to simplify protein determination in membrane and lipoprotein samples. Anal. Biochem. **87**:206–210.
31. **Meinhardt, S. W., P. J. Kiley, S. Kaplan, A. R. Crofts, and S. Harayama.** 1985. Characterization of light-harvesting mutants of *Rhodopseudomonas sphaeroides*. I. Measurement of the efficiency of energy transfer from light-harvesting complexes to the reaction center. Arch. Biochem. Biophys. **236**:130–139.
32. **Mejbaum, W.** 1939. A more sensitive pentose measurement, especially for derivatives of adenylic acid. Hoppe-Seyler's Z. Physiol. Chem. **258**:117–120.
33. **Messing, J.** 1979. A multi-purpose cloning system based on the single-stranded DNA bacteriophage M13. Recomb. DNA Tech. Bull. **2**:43–48.
34. **Nano, F. E., and S. Kaplan.** 1984. Plasmid rearrangements in the photosynthetic bacterium *Rhodopseudomonas sphaeroides*. J. Bacteriol. **158**:1094–1103.
35. **Newbury, S. F., N. H. Smith, and C. F. Higgins.** 1987. Differential mRNA stability controls relative gene expression within a polycistronic operon. Cell **51**:1131–1143.
36. **Newbury, S. F., N. H. Smith, E. C. Robinson, I. D. Hiles, and C. F. Higgins.** 1987. Stabilization of translationally active mRNA by prokaryotic REP sequences. Cell **48**:297–310.
37. **Prince, R. C., E. Davidson, C. E. Haith, and F. Daldal.** 1986. Photosynthetic electron transfer in the absence of cytochrome c_2 in *Rhodopseudomonas capsulata*: cytochrome c_2 is not essential for electron flow from the cytochrome bc_1 complex to the photochemical reaction center. Biochemistry **25**:5208–5214.
38. **Simon, R., U. Priefer, and A. Pühler.** 1983. A broad host range mobilization system for in vivo genetic engineering: transposon mutagenesis in Gram-negative bacteria. Bio/Technology **1**:37–45.
39. **Southern, E.** 1979. Gel electrophoresis of restriction fragments. Methods Enzymol. **68**:152–176.
40. **Stern, D. B., and W. Gruissem.** 1987. Control of plastid gene expression: 3′ inverted repeats act as mRNA processing and stabilizing elements, but do not terminate transcription. Cell **51**: 1145–1157.
41. **Tai, S. P., and S. Kaplan.** 1985. Intracellular localization of phospholipid transfer activity in *Rhodopseudomonas sphaeroides* and a possible role in membrane biogenesis. J. Bacteriol. **164**:181–186.
42. **Thomas, P. S.** 1983. Hybridization of denatured RNA transferred or dotted to nitrocellulose paper. Methods Enzymol. **100**: 255–266.
43. **Tinoco, I., P. N. Borer, B. Dengler, M. D. Levine, O. C. Uhlenbeck, D. M. Crothers, and J. Gralla.** 1973. Improved estimation of secondary structure in ribonucleic acids. Nature (London) New Biol. **246**:40–41.
44. **Van Niel, C. B.** 1944. The culture, general physiology, and classification of the non-sulfur purple and brown bacteria. Bacteriol. Rev. **8**:1–118.
45. **Vieira, J., and J. Messing.** 1982. The pUC plasmids, an M13mp7-derived system for insertion mutagenesis and sequencing with synthetic universal primers. Gene **19**:259–268.
46. **White, B. A., and F. C. Bancroft.** 1982. Cytoplasmic dot hybridization: simple analysis of relative mRNA levels in multiple small cell or tissue samples. J. Bio. Chem. **257**:8569–8572.
47. **Williams, J. C., L. A. Steiner, G. Feher, and M. I. Simon.** 1984. Primary structure of the L subunit of the reaction center of *Rhodopseudomonas sphaeroides*. Proc. Natl. Acad. Sci. USA **81**:7303–7308.
48. **Williams, J. C., L. A. Steiner, R. C. Ogden, M. I. Simon, and G. Feher.** 1983. Primary structure of the M subunit of the reaction center from *Rhodopseudomonas sphaeroides*. Proc. Natl. Acad. Sci. USA **80**:6505–6509.
49. **Wright, J. K., and P. Overath.** 1984. Purification of the lactose: H^+ carrier of *Escherichia coli* and characterization of galactoside binding and transport. Eur. J. Biochem. **138**:497–508.
50. **Yanisch-Perron, C., J. Vieira, and J. Messing.** 1985. Improved M13 phage cloning vectors and host strains: nucleotide sequences of the M13mp18 and pUC19 vectors. Gene **33**:103–119.
51. **Yanofsky, C.** 1988. Transcription attenuation. J. Biol. Chem. **263**:609–612.
52. **Zhu, Y. S., and S. Kaplan.** 1985. Effects of light, oxygen, and substrates on steady-state levels of mRNA coding for ribulose 1,5-bisphosphate carboxylase and light-harvesting and reaction center polypeptides in *Rhodopseudomonas sphaeroides*. J. Bacteriol. **162**:925–932.
53. **Zhu, Y. S., P. J. Kiley, T. J. Donohue, and S. Kaplan.** 1986. Origin of the mRNA stoichiometry of the *puf* operon in *Rhodobacter sphaeroides*. J. Biol. Chem. **261**:10366–10374.